

A Relative Study on Two-photon Absorption Properties of C₆₀ and C₇₀

ZHOU, Xin^a(周新) REN, Ai-Min^a(任爱民) FENG, Ji-Kang^{*a,b}(封继康)
LIU, Xiao-Juan^a(刘孝娟)

^a State Key Laboratory of Theoretical and Computational Chemistry, Institute of Theoretical Chemistry,
Jilin University, Changchun, Jilin 130023, China

^b College of Chemistry, Jilin University, Changchun, Jilin 130023, China

We have theoretically investigated the one- and two-photon absorption properties of C₆₀ and C₇₀ using the ZINDO method. From the results it is suggested that the one-photon absorption spectra are in agreement with the experimental observations. It is found that the maximum TPA cross section of C₇₀ is more than twice that of C₆₀, which is consistent with the experimental results. A notable point is that the TPA process of C₆₀ is different from that of C₇₀ as well as other ordinary conjugated molecules.

Keywords two-photon absorption, ZINDO-SOS, C₆₀, C₇₀

Introduction

Cage-like carbon clusters, fullerenes, are the subject of wide interdisciplinary interest in materials science. C₆₀ was first found in the laser desorption mass spectroscopy of carbon in 1985,¹ but the discovery of mass production of fullerenes by Krätschmer *et al.*² in 1990 opened the field to a large number of new workers interested in this class of materials. Amongst the various kinds of fullerenes, C₆₀ and C₇₀ are the most abundant and have been extensively studied. The three-dimensional cage structure¹ of fullerene provides plenty of delocalized π electrons, which is of particular interest for the nonlinear optical response. Many researchers have examined theoretically and observed experimentally the superconductivity, magnetic ordering, photo-physical and excited-state kinetic properties and optical limiting properties.³⁻⁵ However, less attention has been paid to the two-photon absorption (TPA) properties of C₆₀ and C₇₀. The TPA process considered here involves the simultaneous absorption of two photons, and the transition probability for absorption of two identical photons is proportional to I^2 , where I is the intensity of the laser pulse. The TPA phenomena of materials have now received more and more consideration for the potentially practical applications such as upconverted lasing,⁶⁻⁸ optical power limiting,⁹⁻¹¹ photodynamic therapy,¹² and three-dimensional (3D) microfabrication.¹³⁻¹⁵ These applications have stimulated research on the design, synthesis and characterization of new molecules with large TPA cross sections. On the basis of the observations by Albota *et al.*,¹⁶ it was found that those

molecules having large TPA cross section contain both donors and acceptors that are connected to each other via conjugated polyenes. Later on, there appeared several ways to optimize the nonlinear optical (NLO) characteristics of such a chromophore, such as increasing the strength of the donor and acceptor groups,^{17,18} modifying the nature of the conjugated bridge^{19,20} and increasing the conjugated length of the bridge. In contrast to the extensive investigation on the structure-TPA relationship of the dipolar and quadrupolar molecules, recently, reports on the TPA property of the octupolar molecule with multi-branched structure became more and more.^{21,22} Most of the studied molecules possess one-dimensional structure or two-dimensional structure, but the researches on the TPA properties of three-dimensional fullerenes such as C₆₀ and C₇₀ are lacked. It is known that C₆₀ and C₇₀ exhibit large third-order NLO response and the TPA cross section $\delta(\omega)$ of materials can be directly related to the imaginary part of the third-order optical susceptibility. According to this relationship, one can anticipate that C₆₀ and C₇₀ should have large TPA cross sections. So in this paper, we studied the TPA properties of C₆₀ and C₇₀ theoretically using the ZINDO method and analyzed the differences between them.

Theoretical methodology

The TPA process corresponds to simultaneous absorption of two photons. The TPA efficiency of an organic molecule, at optical frequency $\omega/2\pi$, can be characterized by the TPA cross-section $\delta(\omega)$. It can be

* E-mail: jikangf@yahoo.com

Received September 16, 2003; revised and accepted March 1, 2004.

Project supported by the National Natural Science Foundation of China (Nos. 20273023, 90101026) and the Key Laboratory for Supramolecular Structure and Material of Jilin University.

directly related to the imaginary part of the second hyperpolarizability $\gamma(-\omega; \omega, \omega, -\omega)$ by:¹⁶

$$\delta(\omega) = \frac{8\pi^2 \hbar \omega^2}{n^2 c^2} L^4 \text{Im} \gamma(-\omega; \omega, \omega, -\omega) \quad (1)$$

where \hbar is Planck's constant divided by 2π , n is the refractive index of medium, c is the speed of light, L is a

$$\begin{aligned} \gamma_{ijkl}(-\omega_\sigma; \omega_1, \omega_2, \omega_3) = & \frac{4\pi^3}{3\hbar^3} P(i, j, k, l; -\omega_\sigma; \omega_1, \omega_2, \omega_3) \cdot \\ & \left[\sum_{m \neq o} \sum_{n \neq o} \sum_{p \neq o} \frac{\langle o | \mu_i | m \rangle \langle m | \bar{\mu}_j | n \rangle \langle n | \bar{\mu}_k | p \rangle \langle p | \mu_l | o \rangle}{(\omega_{mo} - \omega_\sigma - i\Gamma_{mo})(\omega_{no} - \omega_2 - \omega_3 - i\Gamma_{no})(\omega_{po} - \omega_3 - i\Gamma_{po})} - \right. \\ & \left. \sum_{m \neq o} \sum_{n \neq o} \frac{\langle o | \mu_i | m \rangle \langle m | \mu_j | o \rangle \langle o | \mu_k | n \rangle \langle n | \mu_l | o \rangle}{(\omega_{mo} - \omega_\sigma - i\Gamma_{mo})(\omega_{no} - \omega_3 - i\Gamma_{no})(\omega_{no} + \omega_2 - i\Gamma_{no})} \right] \end{aligned} \quad (2)$$

where $P(i, j, k, l; -\omega_\sigma; \omega_1, \omega_2, \omega_3)$ is a permutation operator defined in such a way that for any permutation of (i, j, k, l) , an equivalent permutation of $(-\omega_\sigma; \omega_1, \omega_2, \omega_3)$ is made simultaneously; $\omega_\sigma = \omega_1 + \omega_2 + \omega_3$ is the polarization response frequency; $\omega_1, \omega_2, \omega_3$ indicate the frequencies of the perturbing radiation fields (considering the degenerate TPA, $\omega_1 = \omega_2 = \omega$ and $\omega_3 = -\omega$); i, j, k and l correspond to the molecular axes x, y and z ; m, n and p denote excited states and o , the ground state; μ_j is the j (= x, y, z)*th* component of the dipole operator; $(\langle m | \bar{\mu}_j | n \rangle = \langle m | \mu_j | n \rangle - \langle o | \mu_j | o \rangle)$; $(\hbar/2\pi)\omega_{mo}$ is the transition energy between the m and o states and Γ_{mo} is the damping factor of excited state m . Considering that the higher the excited state is, and the shorter the lifetime is, the Γ_{mo} is expressed as follows:²⁵

$$\Gamma_{mo} = 0.08 \times \frac{\omega_{mo}}{\omega_{1o}} \quad (3)$$

To compare the calculated δ value with the experimental value measured in solution, the orientationally averaged (isotropic) value of γ is evaluated, which is defined as

$$\langle \gamma \rangle = \frac{1}{15} \sum_{i,j} (\gamma_{ijj} + \gamma_{jij} + \gamma_{jji}) \quad i, j = x, y, z \quad (4)$$

In principle, any kind of self-consistent field molecular orbital procedure combined with configuration interaction can be used to calculate the physical values in the above expression. In this paper, the B3LYP/6-31G method was firstly used to calculate molecular equilibrium geometry. Then, the property of electronic excited state was obtained by single and double electron excita-

tion configuration interaction using ZINDO program.

Furthermore, UV-Vis (ground-state one-photon absorption) spectra were provided for predicting TPA properties. Then according to the formulae (1) to (4), the second hyperpolarizability γ and TPA cross section $\delta(\omega)$ of C_{60} and C_{70} were calculated.

local field factor (equal to 1 for vacuum).

The sum-over-states (SOS) expression to evaluate the components of the second hyperpolarizability γ_{ijkl} can be induced out using perturbation theory and density matrix method. By considering a power expansion of the energy with respect to the applied field, the γ_{ijkl} Cartesian components are given by^{23,24}:

tion configuration interaction using ZINDO program. Furthermore, UV-Vis (ground-state one-photon absorption) spectra were provided for predicting TPA properties. Then according to the formulae (1) to (4), the second hyperpolarizability γ and TPA cross section $\delta(\omega)$ of C_{60} and C_{70} were calculated.

Results and discussion

C_{60} is a fascinating, beautiful molecule of high symmetry. Twelve pentagons and twenty hexagons are arranged in a soccer-ball-like structure of about 1 nm diameter that belongs to the icosahedral point group I_h . As far as C_{70} is concerned, its rugby-ball shape can be envisioned either by adding a ring of ten carbon atoms or, equivalently, adding a belt of five hexagons around the equatorial plane of C_{60} molecule which is normal to one of the fivefold axes and suitably rotating the two hemispheres of C_{60} by 36° so that they fit continuously onto the belt hexagons, and its molecular symmetry is D_{5h} . In contrast to C_{60} , which has only one unique carbon site, C_{70} molecule has five inequivalent sites. Hence C_{60} has two unique bond lengths but C_{70} has eight distinct bond lengths. The geometry of C_{60} and C_{70} has been optimized by B3LYP/6-31G method. The result indicates that the independent bond lengths of C_{60} are $R_{6-6} = 0.1397$ nm and $R_{5-6} = 0.14601$ nm, in excellent agreement with the neutron powder diffraction experiment.²⁶ As regard to C_{70} , its optimized geometric parameters are depicted in Figure 1 and listed in Table 1. One can see that our calculation is in accord with the values in literature.²⁷

For C_{60} , Table 2 lists four lowest-lying transitions whose oscillator strength is up to zero and the electronically allowed transitions with none-zero oscillator strength. In terms of C_{70} , the electronically allowed transitions with oscillator strength bigger than 0.01 are tabled in Table 3. Orbital forbidden bands can also appear weakly in solution spectra due to reduction of

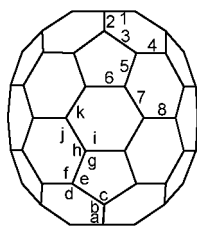


Figure 1 Labels of the optimized geometry of C₇₀.

Table 1 Optimized geometric parameters for C₇₀ (bond lengths in 10⁻¹ nm and bond angles in (°))

Parameter	Value	Value in Ref. 28	Parameter	Value	Value in Ref. 28
1	1.4584	1.4608	c	106.97	106.79
2	1.3990	1.3788	d	120.03	120.07
3	1.4541	1.4553	e	108.53	108.38
4	1.3902	1.3643	f	119.82	120.04
5	1.4553	1.4702	g	107.98	108.22
6	1.4394	1.4174	h	121.43	121.24
7	1.4238	1.4136	i	121.27	121.57
8	1.4762	1.4859	j	118.57	118.53
a	119.74	119.59	k	116.17	115.78
b	120.21	120.34			

Table 2 The calculated and observed one photon absorption spectra of C₆₀

Sym.	$\lambda^{(1)}/\text{nm}$	f	$\lambda^{(1)}_{\text{exp}}/ \text{nm}$	Strength
¹ T _{1g}	538.8	0.00	591	
¹ T _{2g}	534.0	0.00	568	
¹ G _g	522.1	0.00	540	
¹ H _g	469.5	0.00	492	
¹ T _{1u}	354.0	0.01	365	weak
¹ T _{1u}	295.7	0.06	328	medium
¹ T _{1u}	245.0	1.08	256	strong
¹ T _{1u}	229.9	1.02	227	shoulder
¹ T _{1u}	208.3	7.34	211	strong

^a From Ref. 29.

local symmetry resulting from solute-solvent interactions. Thus it can be seen that the disagreement between theoretical calculations and experimental observations is understandable. The gained strong peaks are in good agreement with observed values²⁸ and also consistent with the previous results of our group.²⁹

Now we turn our attention to the calculation results of TPA properties of C₆₀ and C₇₀. According to expressions (1)–(4), we compiled a program to calculate the third-order optical susceptibility γ and the TPA cross section $\delta(\omega)$. The absorption of light by matter is a consequence of the interaction of an electromagnetic

Table 3 The calculated and observed one photon absorption spectra of C₇₀

Sym.	$\lambda^{(1)}/\text{nm}$	f	$\lambda^{(1)}_{\text{exp}}/ \text{nm}$	Strength
¹ E ₁ '	485.6	0.05	469	medium
¹ A ₂ ''	390.8	0.13	378	medium
¹ E ₁ '	381.5	0.12		
¹ A ₂ ''	360.7	0.06		
¹ E ₁ '	332.1	0.08	359	medium
¹ A ₂ ''	313.0	0.05	331	medium
¹ E ₁ '	310.8	0.01	313	weaker
¹ E ₁ '	298.6	0.01		
¹ A ₂ ''	289.3	0.03		
¹ E ₁ '	277.7	0.01		
¹ E ₁ '	267.2	0.13		
¹ E ₁ '	263.3	0.36		
¹ A ₂ ''	262.2	0.53		
¹ A ₂ ''	254.9	0.03		
¹ E ₁ '	248.1	0.07		
¹ E ₁ '	244.1	0.02		
¹ E ₁ '	243.8	0.05		
¹ E ₁ '	240.9	0.03		
¹ E ₁ '	234.1	0.26		
¹ A ₂ ''	226.3	8.30	236	strong
¹ E ₁ '	225.7	1.17		
¹ A ₂ ''	223.3	1.55		
¹ E ₁ '	208.0	6.04	215	strong
¹ A ₂ ''	201.4	1.06		
¹ E ₁ '	190.0	0.15		

^a From Ref. 29.

field with optically induced electric dipoles in a molecule. For the molecule like C₆₀ that has central symmetry, a change in the parity between the initial and final states (wave functions) is required for every photon involved in the transition for electric dipole transitions. Thus the selection rule for TPA is different from that of OPA. One change of parity is required for a one-photon transition, while two-photon transitions must have initial and final states with the same parity. Because the ground state of C₆₀ is A_g symmetry, according to the selection rule, we select all excited states with g symmetry as possible TPA final states to calculate TPA cross sections. The frequency dependent curve of TPA cross sections for C₆₀ is shown in Figure 2. However, for the molecule without a center of inversion symmetry such as C₇₀, every state is of mixed parity and hence all electronic states involving any number of photons are allowed. So we consider every state as the possibility of being the TPA final state to depict the TPA spectrum of C₇₀ (displayed in Figure 3). As can be seen in Figure 2, for C₆₀, at 518 nm, the TPA cross section gives a maximum, $995.7 \times 10^{-50} \text{ cm}^4 \cdot \text{s}/\text{photon}$. The result is in good agreement with the observed result of Refs. 30 and 31. The states corresponding to the peak TPA cross section

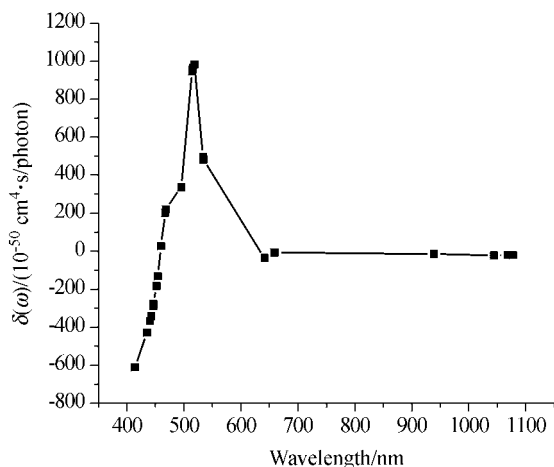


Figure 2 TPA spectrum for C_{60}

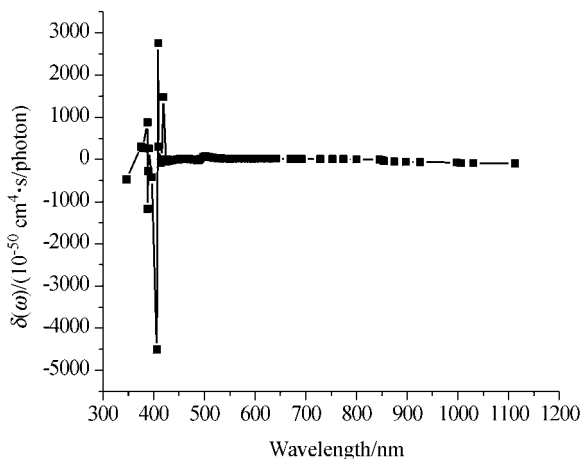


Figure 3 TPA spectrum of C_{70}

have 1H_g symmetry, which is in line with the standpoint mentioned in Ref. 31. With regard to C_{70} , as shown in Figure 3, the TPA spectrum is much more complicated than that of C_{60} . There are four TPA peaks in the Figure 3 compared with only one TPA peak in the TPA spectrum of C_{60} . Because the reduced symmetry of C_{70} allows at most for doubly degenerate states while C_{60} allows five-fold degeneracies, the number of possible

TPA final states of C_{70} is more than that of C_{60} . In the four peaks of TPA spectrum of C_{70} , the maximum TPA cross section value is $2757.5 \times 10^{-50} \text{ cm}^4 \cdot \text{s}/\text{photon}$ at 408.6 nm and the corresponding excited state is ${}^1A_2''$ symmetry. This maximum TPA cross section of C_{70} is about 2.7 times larger than that of C_{60} . It is suggested in the Refs. 32 and 33 that the third-order optical susceptibility γ of C_{70} is more than twice that of C_{60} . On the basis of the direct proportional relationship between the imaginary part of the third-order optical susceptibility and TPA cross section, one can dope out that the difference between the TPA cross sections of C_{60} and C_{70} is more than twice. Obviously, our calculations are in good agreement with the experimental observations. This difference results from the fact that electron transfer within a larger volume favors the maximum TPA cross section of molecule.

It is interesting to point out another difference between C_{60} and C_{70} on the TPA process. For ordinary conjugated molecules, the position and relative strength of the two-photon resonance are to be predicted using the following simplified form—three-state approximation of the SOS expression:^{16,23}

$$\delta \propto \frac{M_{0k}^2 M_{kn}^2}{(E_{0k} - E_{0n} / 2)^2} \quad (5)$$

where M_{ij} is the transition dipole moment from the state i to j ; E_{ij} is the corresponding excitation energy, and the subscripts 0, k and n refer to the ground state S_0 , the virtual intermediate state S_k and the TPA final state S_n respectively. This formula can considerably facilitate a search and design of new molecules with strongly enhanced TPA, because it is a simple relationship between the TPA cross section value and some usual linear absorption parameters. For ordinary conjugated molecules with large TPA cross sections, the intermediate state of TPA (namely the final state of OPA) should locate lower than the final state of TPA. However, for C_{60} , the intermediate state of TPA corresponding to the first strong OPA peak appears to be higher state than the final state of TPA (displayed in Figure 4 (a)). As to C_{70} , the similar

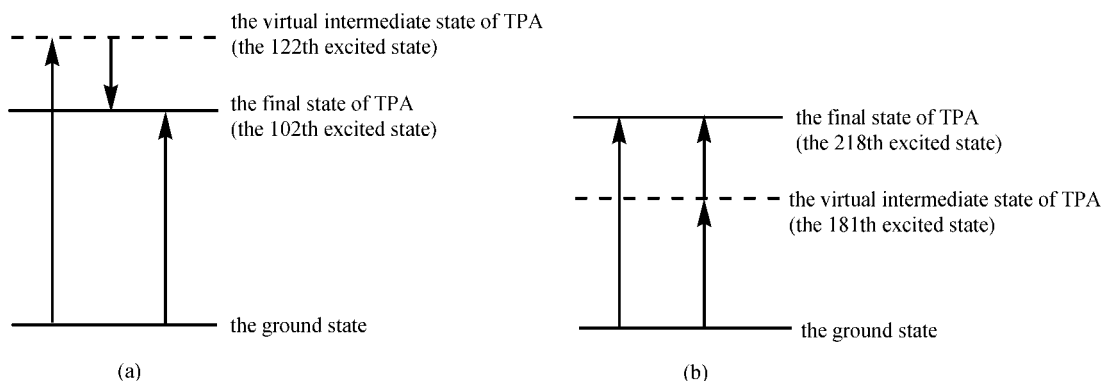


Figure 4 Sketch map of the two-photon absorption of (a) C_{60} and (b) C_{70} .

TPA process to the ordinary conjugated molecules with large TPA cross sections is exhibited and shown in Figure 4 (b), that is, the TPA intermediate state (the first strong OPA peak) lies lower than the final state of TPA. This distinctness can be explained by analyzing the relationship between the OPA and TPA parameters in two fullerenes. As far as C₆₀ is concerned, the first OPA with oscillator strength equal to 0.01 is 365 nm, which is shorter than the maximum TPA wavelength 518 nm. With respect to C₇₀, the maximum TPA peak appears at 408.6 nm, which is shorter than 485.6 nm—the first OPA with oscillator strength up to 0.05.

Conclusion

In this paper, we have performed the theoretical research on the TPA properties of C₆₀ and C₇₀. The calculated TPA cross section peak of C₇₀ ($2757.5 \times 10^{-50} \text{ cm}^4 \cdot \text{s} / \text{photon}$) is about 2.7 times as large as that of C₆₀ ($995.7 \times 10^{-50} \text{ cm}^4 \cdot \text{s} / \text{photon}$), which is in line with results in literatures. It is notable that, the TPA processes of both are entirely different on the basis of the concept of three-state approximation of the SOS expression. The interesting differences are attributed to the dissimilitude in the contrastive relation between OPA and TPA parameters of C₆₀ and C₇₀.

References

- Kroto, H. W.; Heath, J. R.; O'Brien, S. C.; Curl, R. F.; Smalley, R. E. *Nature* **1985**, *318*, 162.
- Krätchmer, W.; Lamb, L. D.; Fostiropoulos, K.; Huffman, D. R. *Nature* **1990**, *347*, 354.
- Arvogast, J. N.; Darmanyan, A. P.; Foote, C. S.; Rubin, Y.; Diederich, F. N.; Alvarez, M. M.; Anz, S. J.; Whetten, R. L. *J. Phys. Chem.* **1991**, *95*, 11.
- Sibley, S. D.; Argentine, S. M.; Francis, A. H. *Chem. Phys. Lett.* **1992**, *188*, 187.
- Bindhu, C. V.; Harilal, S. S.; Nampoore, V. P. N.; Vallabhan, C. P. G. *Appl. Phys. B* **2000**, *70*, 429.
- Bhawalkar, J. D.; He, G.-S.; Prasad, P. N. *Rep. Prog. Phys.* **1996**, *59*, 1041.
- He, G.-S.; Zhao, C.-F.; Bhawalkar, J. D.; Prasad, P. N. *Appl. Phys. Lett.* **1995**, *67*, 3703.
- Zhao, C.-F.; He, G.-S.; Bhawalkar, J. D.; Park, C. K.; Prasad, P. N. *Chem. Mater.* **1995**, *7*, 1979.
- Fleitz, P. A.; Sutherland, R. A.; Stroghendl, F. P.; Larson, F. P.; Dalton, L. R. *Proc. SPIE-Int. Soc. Opt. Eng.* **1998**, *3472*, 91.
- He, G.-S.; Bhawalkar, J. D.; Zhao, C.-F.; Prasad, P. N. *Appl. Phys. Lett.* **1995**, *67*, 2433.
- Ehrlich, J. E.; Wu, X.-L.; Lee, I.-Y. S.; Hu, Z.-Y.; Röeckel, H.; Marder, S. R.; Perry, J. W. *Opt. Lett.* **1997**, *22*, 1843.
- Bhawalkar, J. D.; Kumar, N. D.; Zhao, C.-F.; Prasad, P. N. *J. Clin. Laser Med. Surg.* **1997**, *15*, 201.
- Denk, M.; Strickler, J. H.; Webb, W. W. *Science* **1990**, *248*, 73.
- Xu, C. M. J.; Webb, W. W. *Opt. Lett.* **1995**, *20*, 2532.
- Wu, E. S.; Strickler, J. H.; Harrell, W. R.; Webb, W. W. *Proc. SPIE-Int. Soc. Opt. Eng.* **1992**, *1674*, 776.
- Albota, M.; Beljonne, D.; Brédas, J. L.; Ehrlich, J. E.; Fu, J.; Heikal, A. A.; Hess, S. E.; Kogej, T.; Levin, M. D.; Marder, S. R.; McCord-Maughon, D.; Perry, J. W.; Röeckel, H.; Rumi, M.; Subramaniam, G.; Webb, W. W.; Wu, X.; Xu, C. *Science* **1998**, *281*, 1653.
- Cheng, L.-T.; Tan, W.; Stevenson, S. H.; Meridith, G. R.; Rikken, G.; Marder, S. R. *J. Phys. Chem.* **1991**, *95*, 10631.
- Albert, L. D. L.; Das, P. K.; Ramasesha, S. *Chem. Phys. Lett.* **1990**, *168*, 454.
- Jain, M.; Chandrasekhar, J. *J. Phys. Chem.* **1993**, *97*, 4044.
- Matsuzawa, N.; Dixon, D. A. *J. Phys. Chem.* **1992**, *96*, 6332.
- Cho, B. R.; Son, K. H.; Lee, S. H.; Song, Y.-S.; Lee, Y.-K.; Jeon, S.-J.; Choi, J. H.; Lee, H.; Cho, M. *J. Am. Chem. Soc.* **2001**, *123*, 10039.
- Beljonne, D.; Wenseleers, W.; Zojer, E.; Shuai, Z.-G.; Vogel, H.; Pond, S. J. K.; Perry, J. W.; Marder, S. R.; Brédas, J.-L. *Adv. Funct. Mater.* **2002**, *12*, 631.
- Dick, B.; Hochstrasser, R. M.; Trommsdorff, H. P. In *Nonlinear Optical Properties of Organic Molecules and Crystals*, Vol. 2, Eds.: Chemla, D. S.; Zyss, J., Academic Press, Orlando, FL, **1987**, pp. 167—170.
- Orr, B. J.; Ward, J. F. *Mol. Phys.* **1971**, *20*, 513.
- Beljonne, D.; Cornil, J.; Shuai, Z.; Brédas, J. L.; Röhlfing, F.; Bradley, D. D. C.; Torruellas, W. E.; Ricci, V.; Stegeman, G. I. *Phys. Rev. B* **1997**, *55*, 1505.
- David, W. I. F.; Ibberson, R. M.; Mattewman, J. C.; Prasad, K.; Dennis, T. J. S.; Hare, J. P.; Kroto, H. W.; Taylor, R.; Walton, D. R. M. *Nature* **1991**, *12*, 147.
- Baker, J.; Fowler, P. W.; Lazzeretti, P.; Malagoli, M.; Zanasi, R. *Chem. Phys. Lett.* **1991**, *184*, 182.
- Ajie, H.; Alvarez, M. M.; Anz, S. J.; Beck, R. D.; Diederich, F.; Fostiropoulos, K.; Huffman, D. R.; Krätchmer, W.; Rubin, Y.; Schriver, K. E.; Sensharma, D.; Whetten, R. L. *J. Phys. Chem.* **1990**, *94*, 8630.
- Li, J.; Feng, J.-K.; Sun, J.-Z. *Chem. Phys. Lett.* **1993**, *203*, 560.
- Couris, S.; Koudoumas, E.; Ruth, A. A.; Leach, S. *J. Phys. B: At., Mol. Opt. Phys.* **1995**, *28*, 4537.
- Strohkendl, F. P.; Axenson, T. J.; Larsen, R. J.; Dalton, L. R.; Hellwarth, R. W.; Kafafi, Z. H. *J. Phys. Chem. B* **1997**, *101*, 8802.
- Wang, Y.; Cheng, L. *J. Phys. Chem.* **1992**, *96*, 1530.
- Moore, C. E.; Cardelino, B. H.; Wang, X. *J. Phys. Chem.* **1996**, *100*, 4685.